

**Journal of Geodesy**

*Supporting Information for*

**GRACE gravitational measurements of tsunamis after the 2004, 2010, and 2011 great earthquakes**

Khosro Ghobadi-Far (1), Shin-Chan Han (1), Sébastien Allgeyer (2), Paul Tregoning (2), Jeanne Sauber (3), Saniya Behzadpour (4), Torsten Mayer-Gürr (4), Nico Sneeuw (5), Emile Okal (6)

(1) School of Engineering, University of Newcastle, Callaghan, Australia

(2) Research School of Earth Sciences, Australian National University, Canberra, Australia

(3) Geodesy and Geophysics Lab, NASA Goddard Space Flight Center, Greenbelt, Maryland, USA

(4) Institute of Geodesy, Graz University of Technology, Graz, Austria

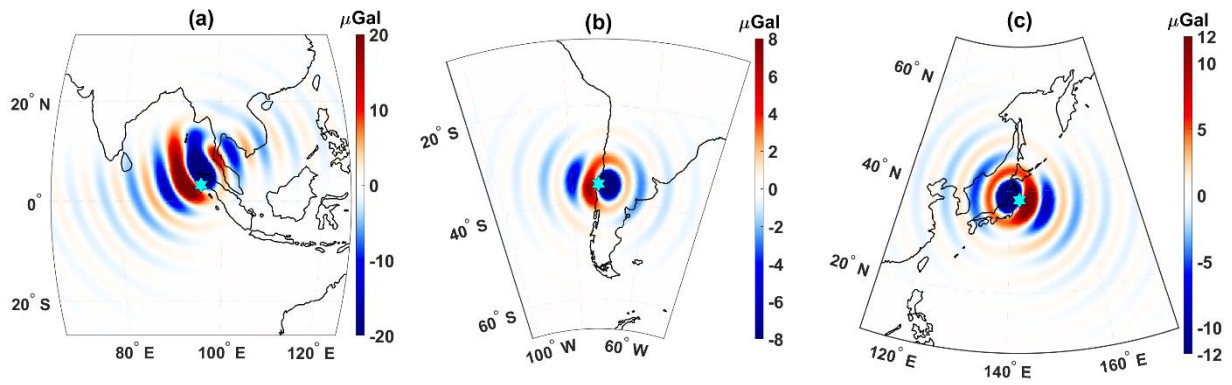
(5) Institute of Geodesy, University of Stuttgart, Stuttgart, Germany

(6) Department of Earth and Planetary Sciences, Northwestern University, Evanston, Illinois, USA

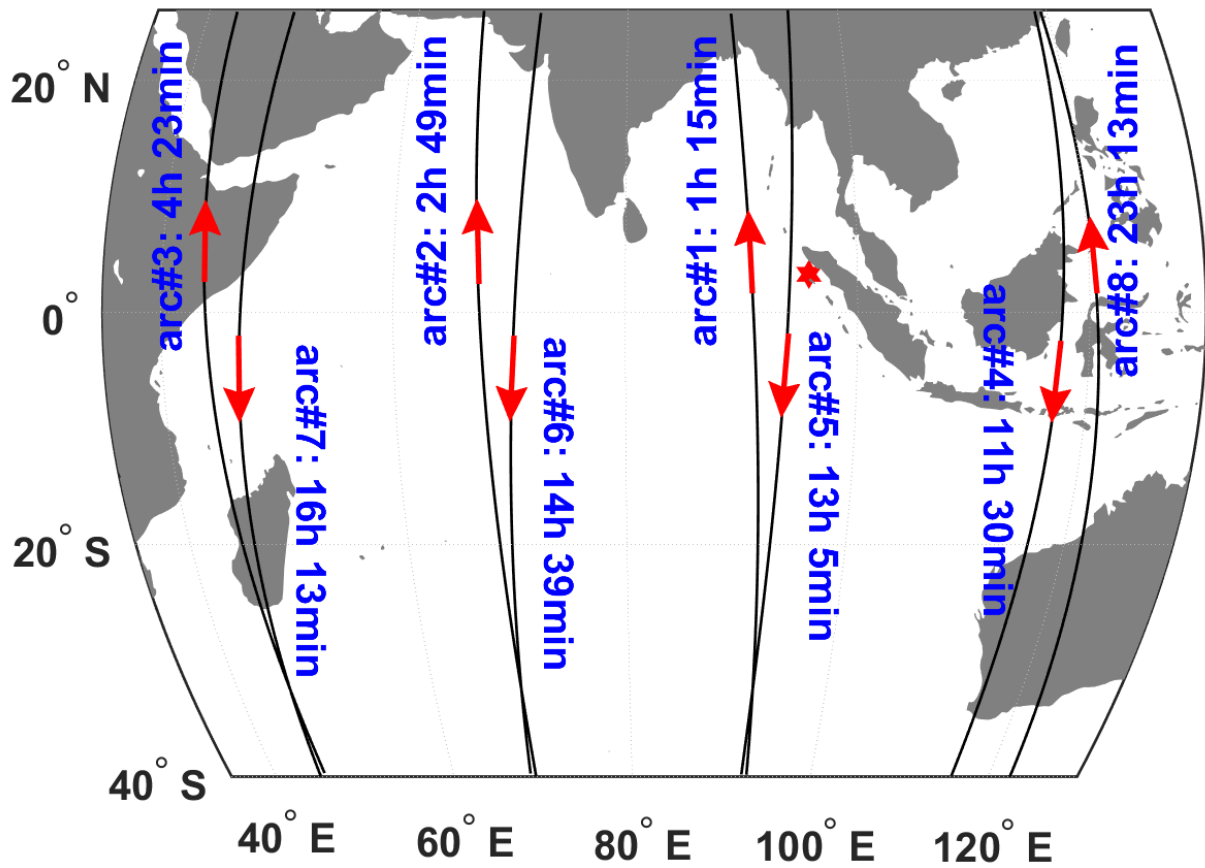
Correspondent: Khosro Ghobadi-Far ([khosro.ghobadifar@uon.edu.au](mailto:khosro.ghobadifar@uon.edu.au))

**Contents of this file:** Figures S1 to S16

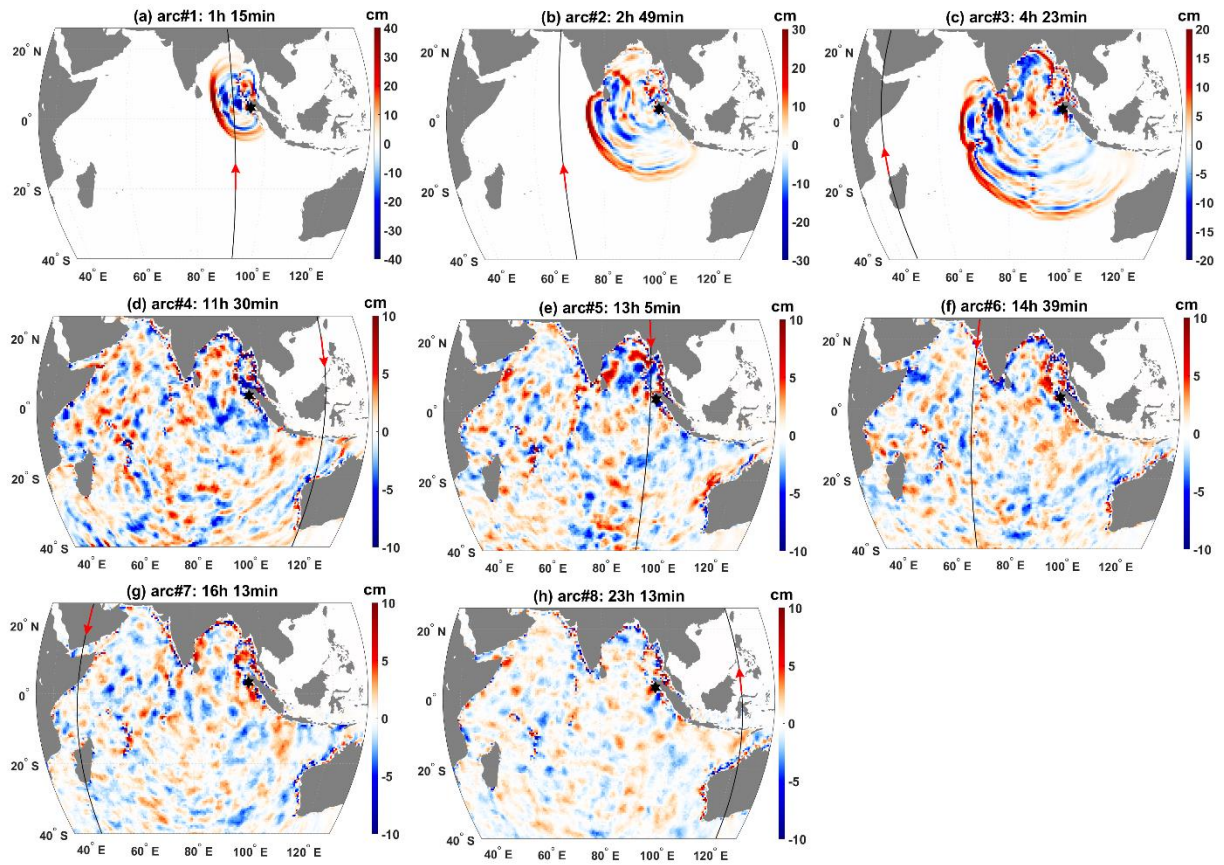
Table S1 and S2



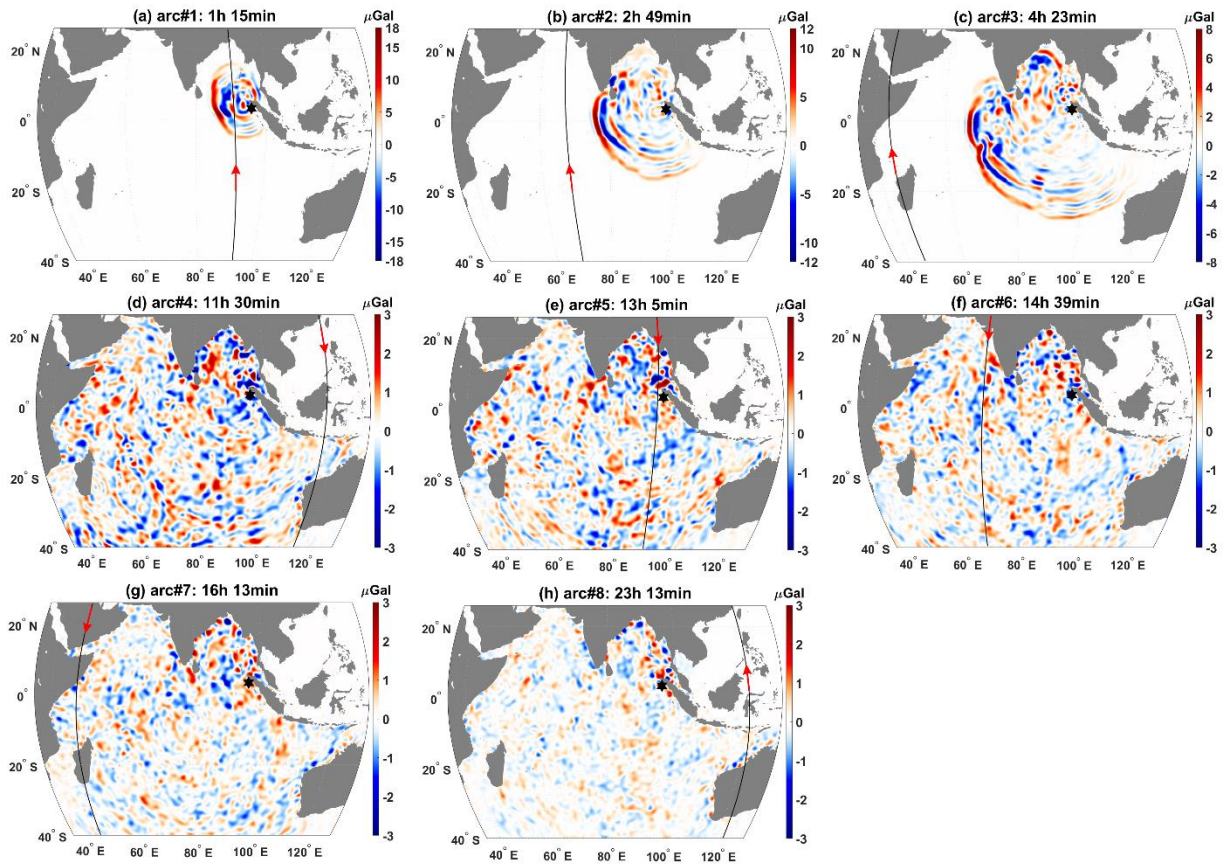
**Figure S1.** Coseismic gravity change in  $\mu\text{Gal}$  ( $10^{-8} \text{ m/s}^2$ ) after the (a) 2004 Sumatra, (b) 2010 Maule, and (c) 2011 Tohoku earthquake obtained from the GRACE monthly gravity solutions by Han et al. 2013. The permanent gravity changes are included in the background models to reduce the effect of coseismic gravity change in the GRACE KBR data. The star indicates the epicenter of the earthquake.



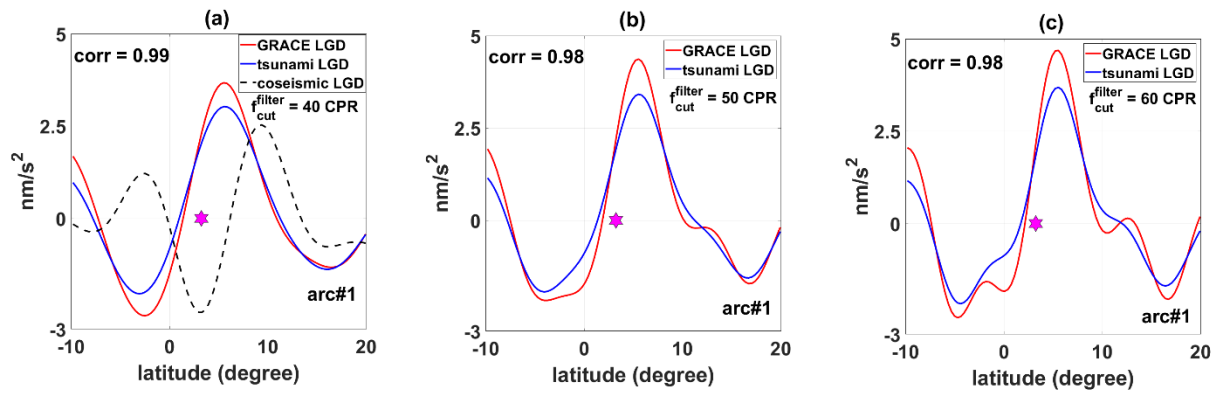
**Figure S2.** GRACE satellites tracks (or arcs) over 24 hours after the 2004 Sumatra earthquake in the region from longitude 35°E to 130°E and latitude 40°S to 26°N. Time of the mid-point for each arc is indicated. Ascending and descending tracks are distinguished by the direction of the arrow. The *red* star indicates the epicenter of the earthquake. Note that closest GRACE ascending and descending tracks (in location) are about 12 hours apart.



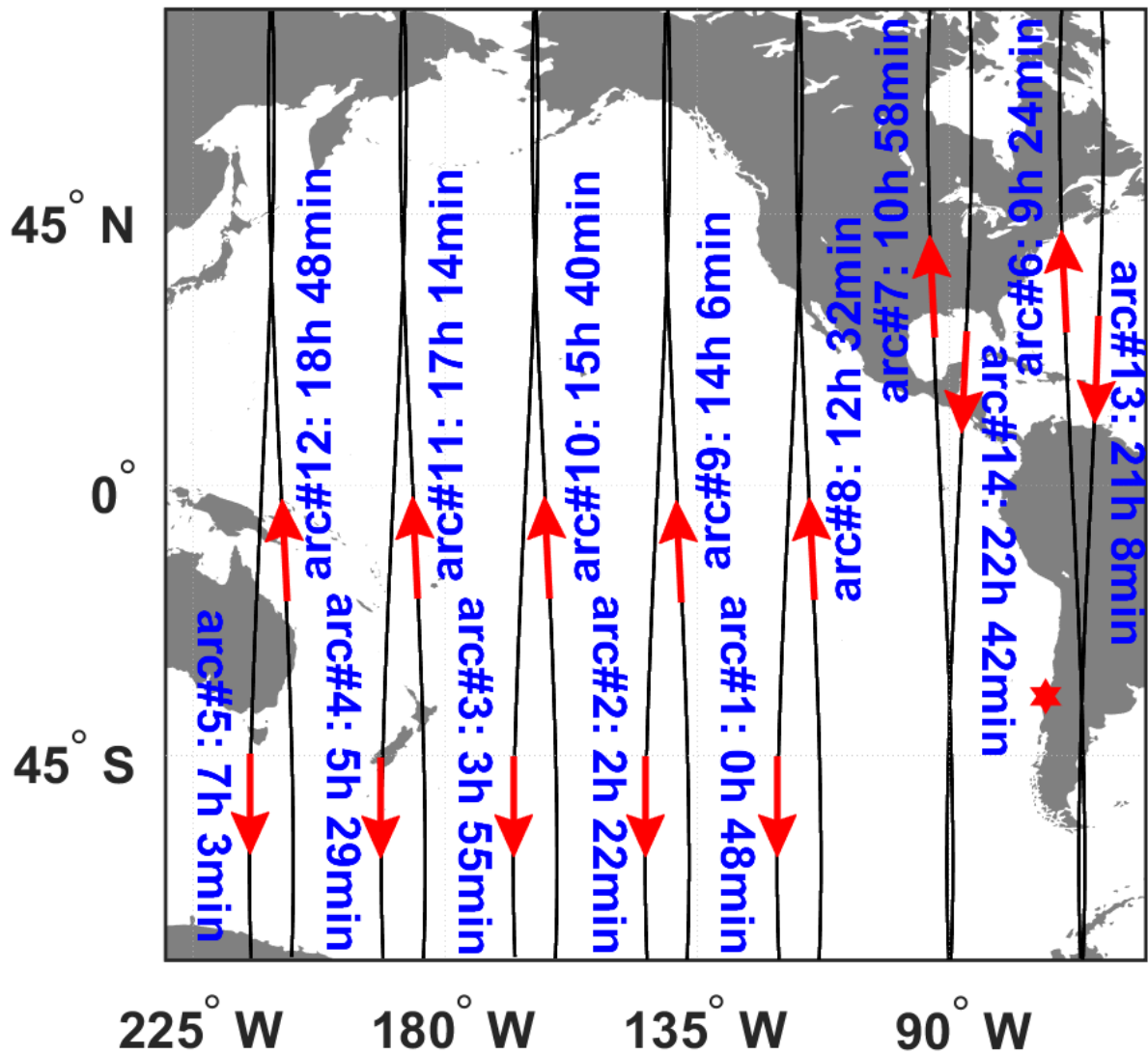
**Figure S3.** GRACE arcs shown in Figure S2 along with the tsunami waves simulated at the time of each arc.



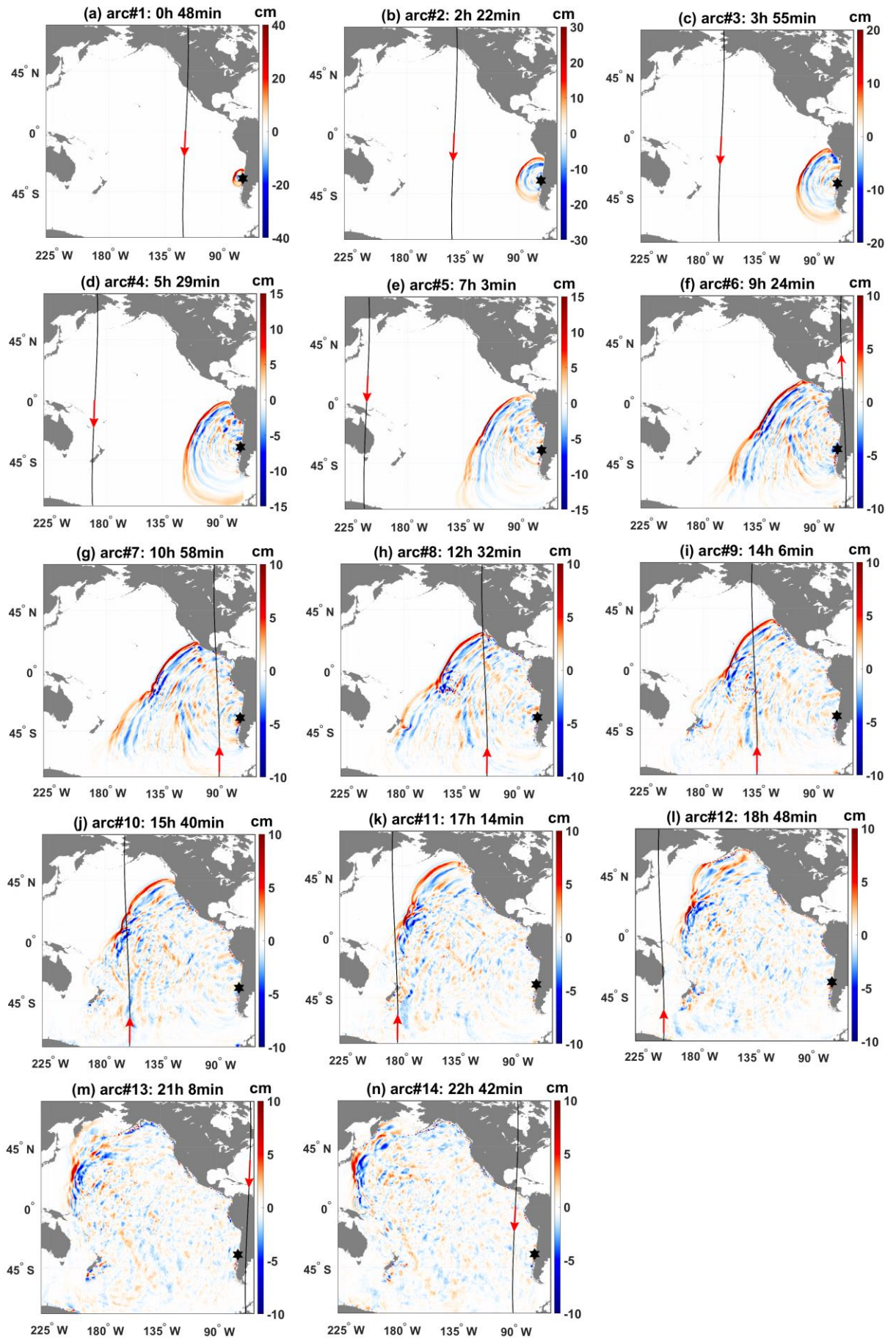
**Figure S4.** Same as Figure S3, but with surface gravity change induced by sea level variation due to tsunami wave propagation. Surface gravity change is represented in terms of gravitational disturbance.



**Figure S5.** Comparison between the GRACE (red) and tsunami (blue) LGD from latitude 10°S and 20°N (where GRACE satellites were passing over the tsunami wave field), both low-pass filtered at (a) 40, (b) 50, and (c) 60 CPR, for arc #1 in Figure S3. The star indicates the epicenter of the earthquake, and the dashed black curve in panel (a) shows the co-seismic gravity change that was modeled out a priori from GRACE data. The correlation between GRACE observations and tsunami model is also indicated.

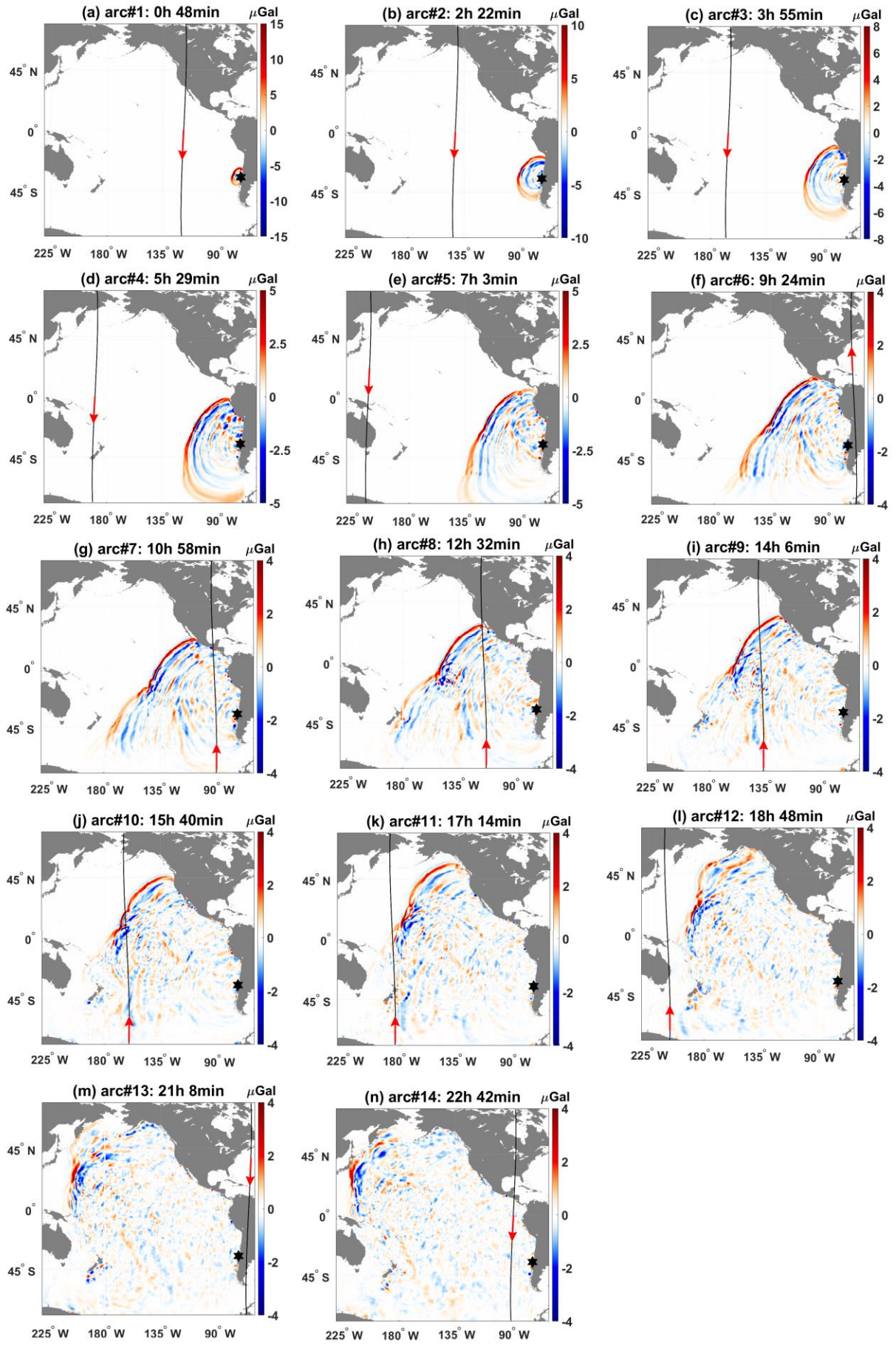


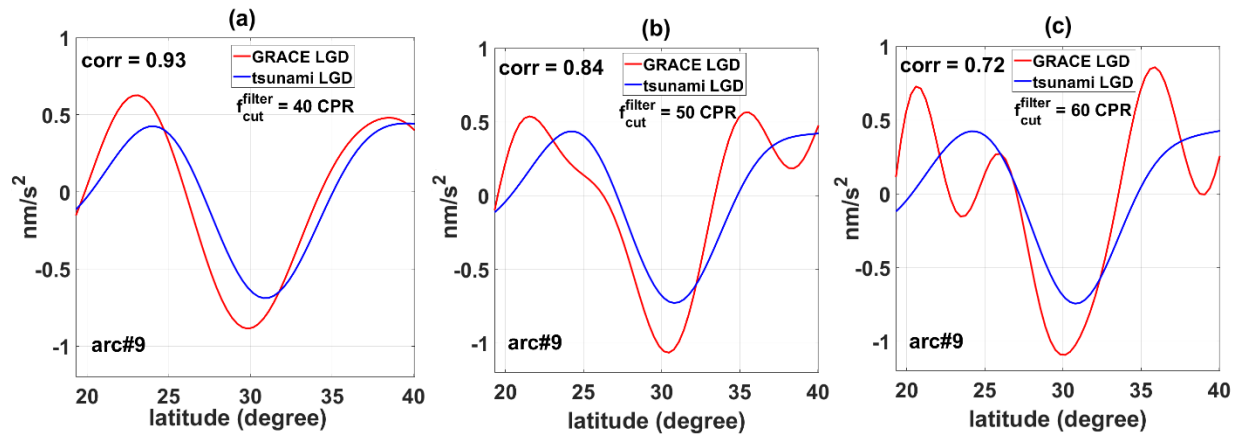
**Figure S6.** GRACE satellites tracks (or arcs) over 24 hours after the 2010 Maule earthquake in the region from longitudes of 130°E to 300°E and latitudes of 70°S to 70°N. Time of the mid-point for each track is indicated. Ascending and descending tracks are distinguished by the direction of the arrow. The *red* star indicates the epicenter of the earthquake.



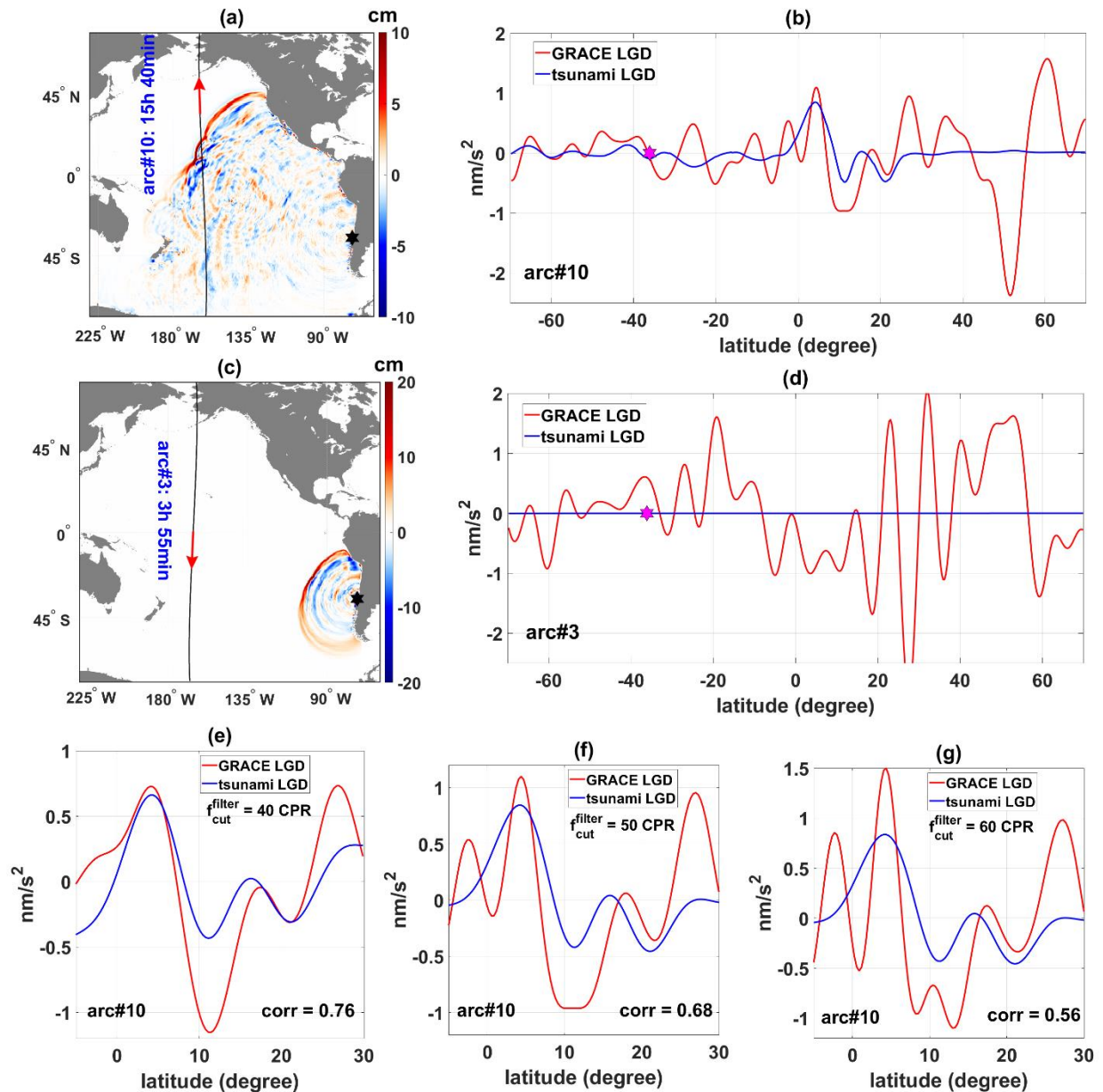
**Figure S7.** GRACE arcs shown in Figure S6 along with the tsunami waves simulated at the time of each track.

Figure S8. Same as Figure S7, but with surface gravity change induced by sea level variation due to tsunami wave propagation.





**Figure S9.** Comparison between the GRACE (red) and tsunami (blue) LGD from latitude 20°N and 40°N (where GRACE satellites were passing over the leading edge of tsunami), both low-pass filtered at (a) 40, (b) 50, and (c) 60 CPR, for arc #9 in Figure S7. The correlation between GRACE observations and tsunami model is also indicated.



**Figure S10.** GRACE possible detection of tsunami triggered by the 2010 Maule earthquake which occurred on 27 February 2010 06:34:11 UTC. **(a)** GRACE ascending track 15 hours and 40 minutes after the earthquake rupture along with the tsunami wave field at the same time. **(b)** Comparison between the GRACE observed (low-pass filtered at 50 CPR, shown in *red*) and tsunami simulated (*blue*) LGD along the ascending track shown in panel (a). **(c)** The closest GRACE descending track over 24 hours after the earthquake which happened 3 hours and 55 minutes after the event along with tsunami wave field at the same time. **(d)** Comparison between the GRACE observed and tsunami simulated LGD along the descending track shown in (c). **(e)**, **(f)**, and **(g)** Comparison of the GRACE (*red*) and tsunami (*blue*) LGD from latitude 5°S to 30°N (where GRACE satellites were passing over the leading edge of tsunami) both low-pass filtered at 40, 50, and 60 CPR, respectively. The star indicates the epicenter of earthquake.

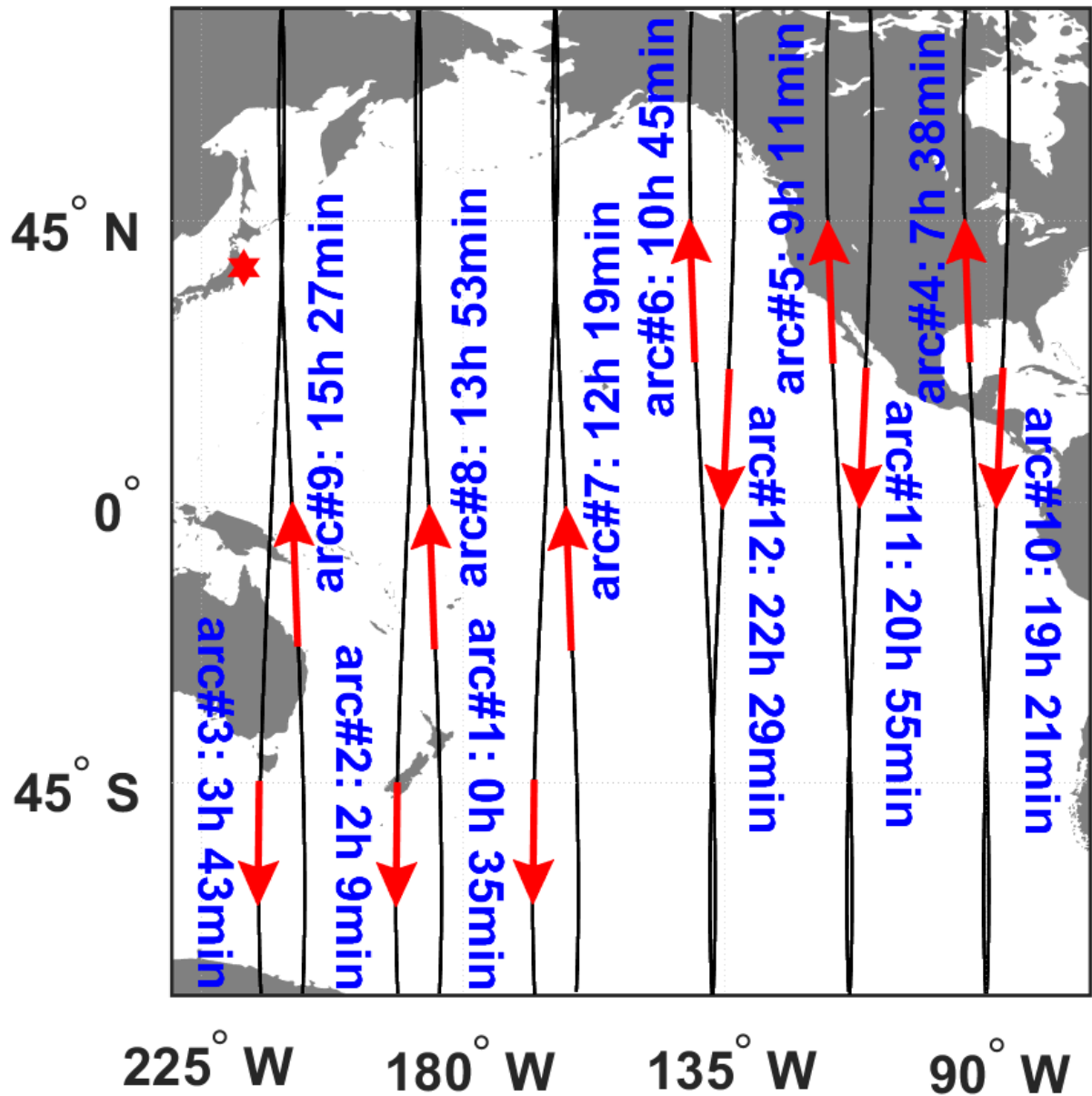


**Figure S11.** GRACE satellites tracks (or arcs) over 24 hours after the 2011 Tohoku earthquake in the region from longitudes of 130°E to 300°E and latitudes of 70°S to 70°N. Time of the mid-point for each track is indicated. Ascending and descending tracks are distinguished by the direction of the arrow. The *red* star indicates the epicenter of the earthquake.

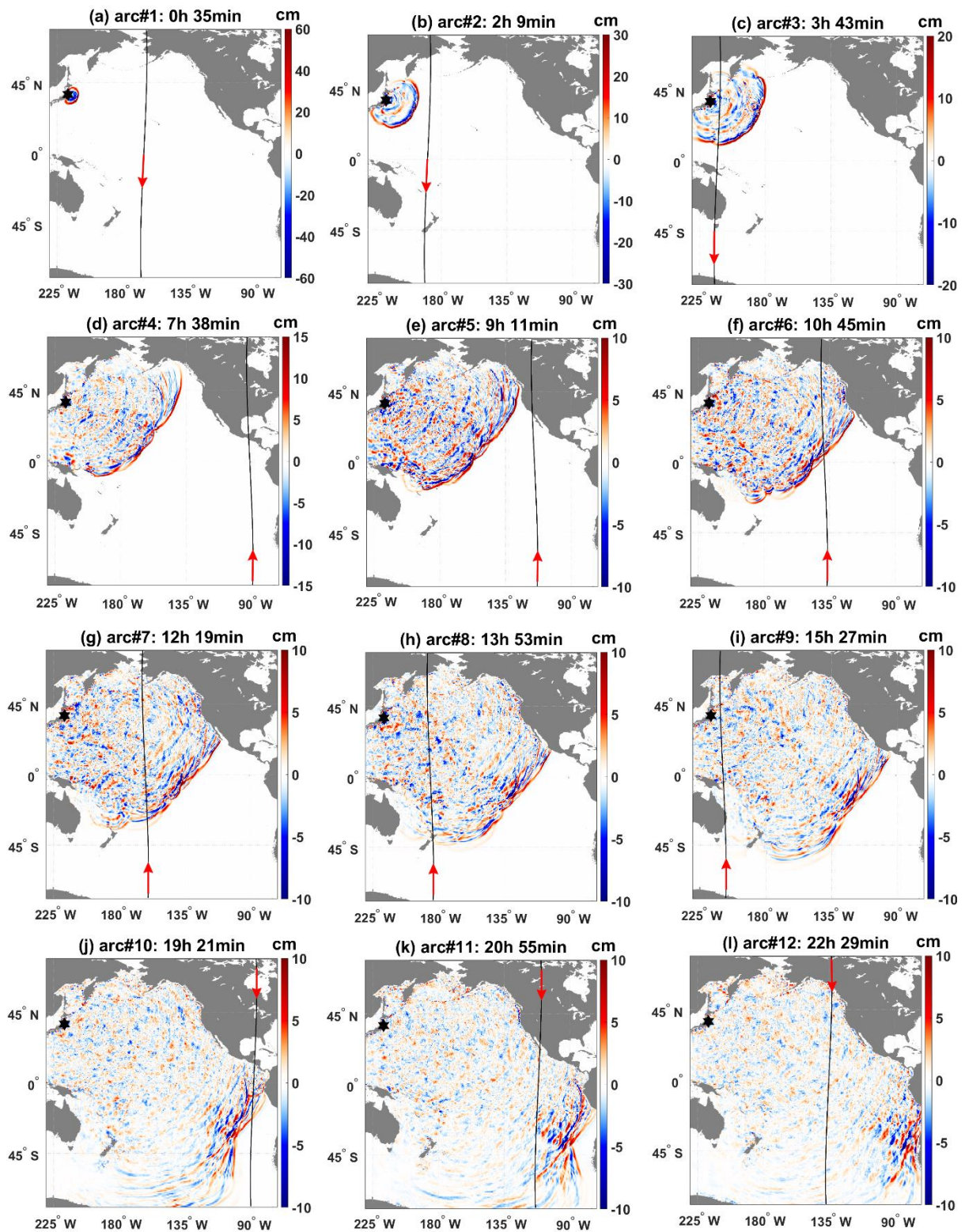


**Figure S12.** GRACE arcs shown in Figure S11 along with the tsunami waves simulated at the time of each arc.

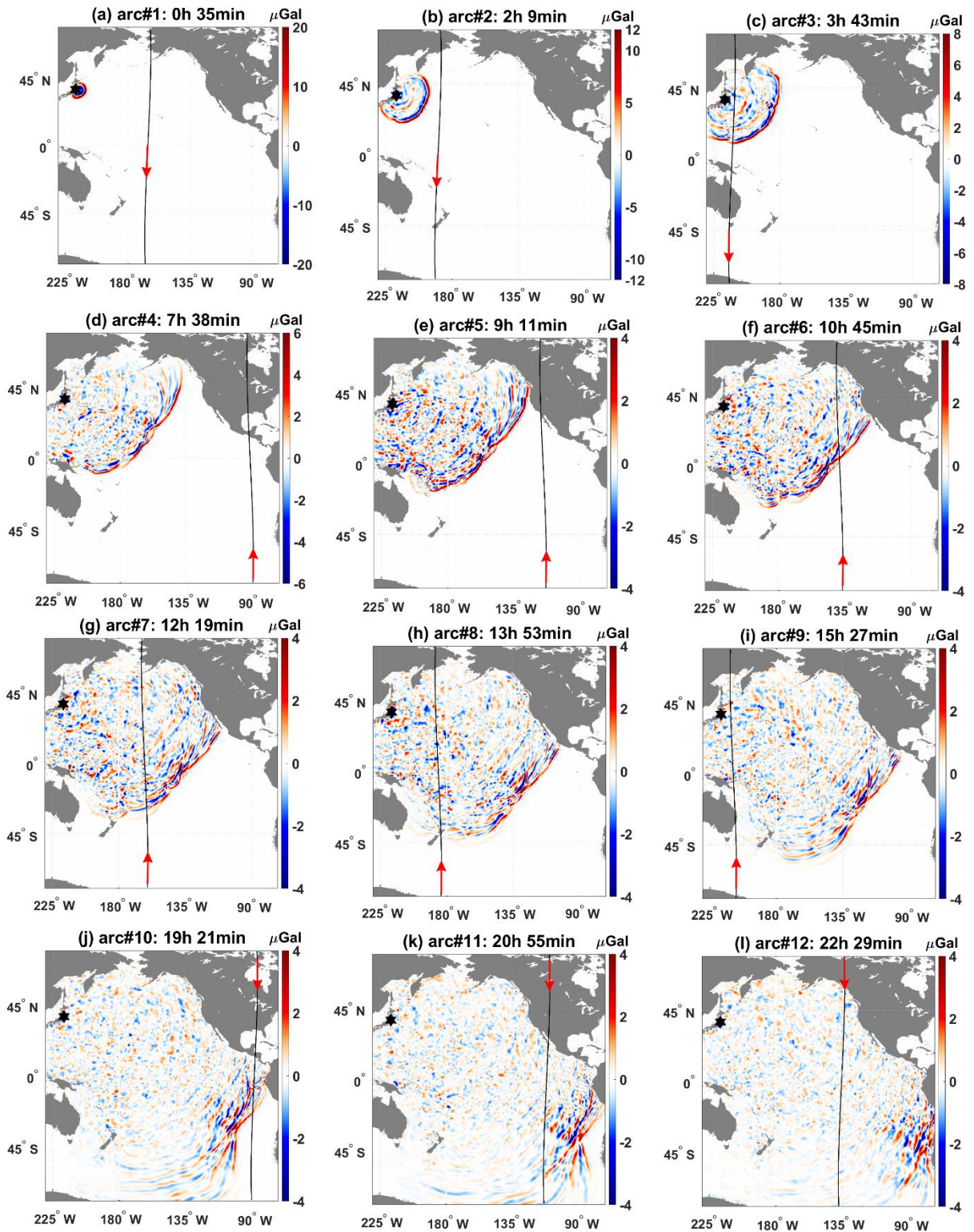


**Figure S13.** Same as Figure S12, but with surface gravity change induced by sea level variation due to tsunami wave propagation.

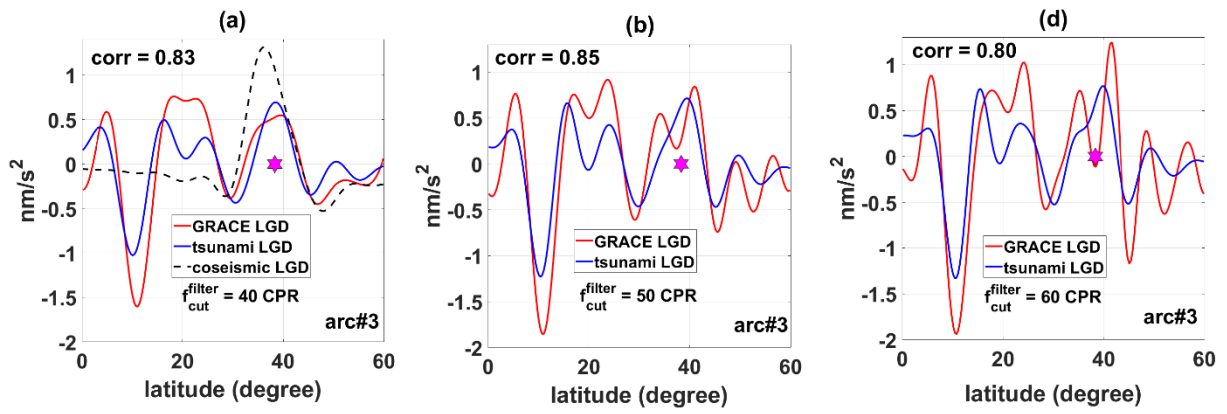


**Figure S14.** Comparison between the GRACE (red) and tsunami (blue) LGD from latitude 0° and 60°N (where GRACE satellites were passing over the tsunami waves), both low-pass filtered at (a) 40, (b) 50, and (c) 60 CPR, for arc #3 in Figure S12. The correlation between GRACE observations and tsunami model is also indicated.

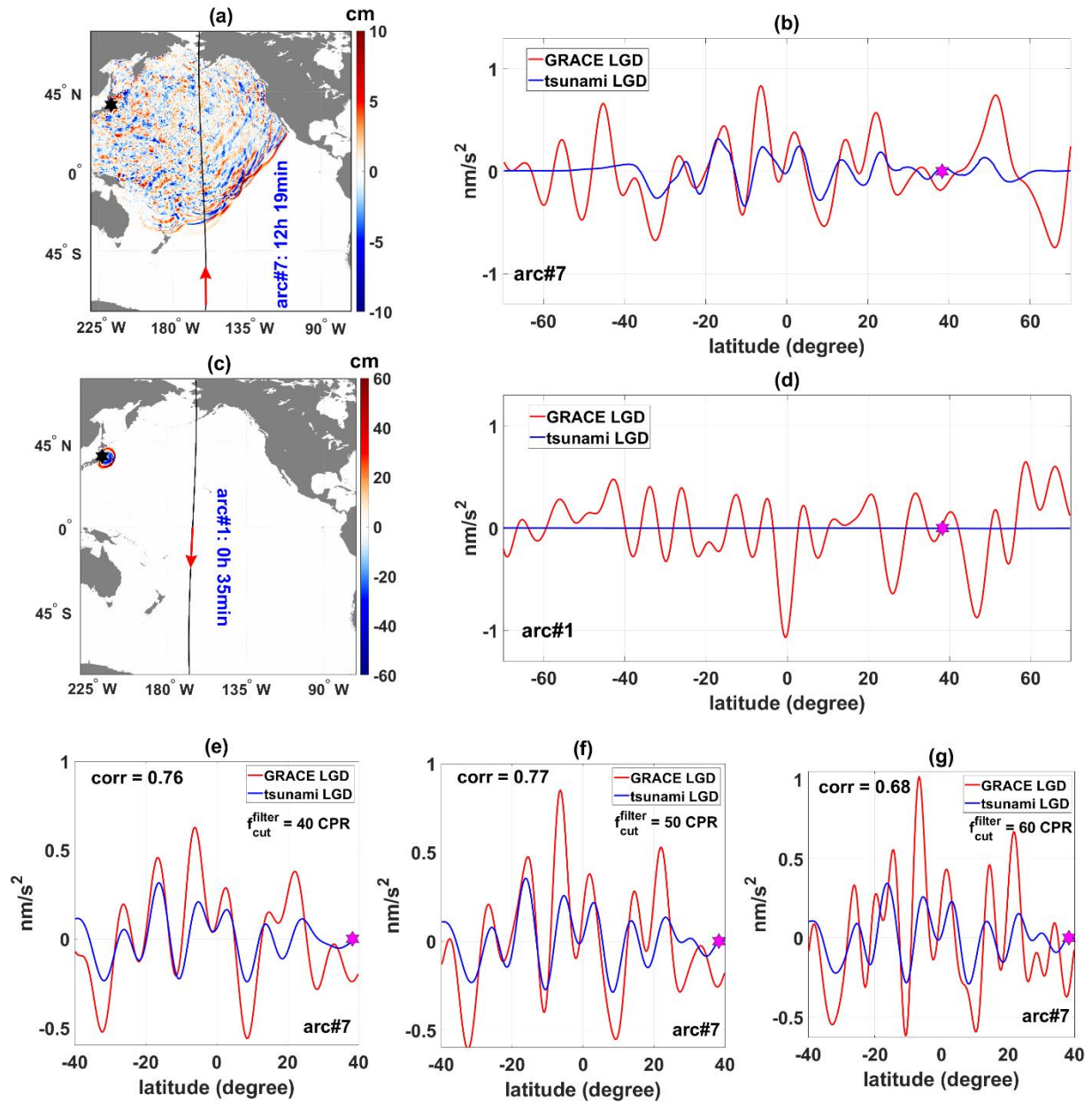


**Figure S15.** GRACE possible detection of tsunami triggered by the 2011 Tohoku earthquake which occurred on 11 March 2011 05:46:24 UTC. **(a)** GRACE ascending track 12 hours and 19 minutes after the earthquake rupture along with the tsunami wave field at the same time. **(b)** Comparison between the GRACE observed (low-pass filtered at 50 CPR, shown in *red*) and tsunami simulated (*blue*) LGD along the ascending track shown in panel (a). **(c)** The closest GRACE descending track over 24 hours after the earthquake which happened 35 minutes after the event along with the tsunami wave field at the same time. **(d)** Comparison between the GRACE observed and tsunami simulated LGD along the descending track shown in (c). **(e)**, **(f)**, and **(g)** Comparison of the GRACE (*red*) and tsunami (*blue*) LGD from latitude 40°S and 40°N both low-pass filtered at 40, 50, and 60 CPR, respectively. The star indicates the epicenter of earthquake.

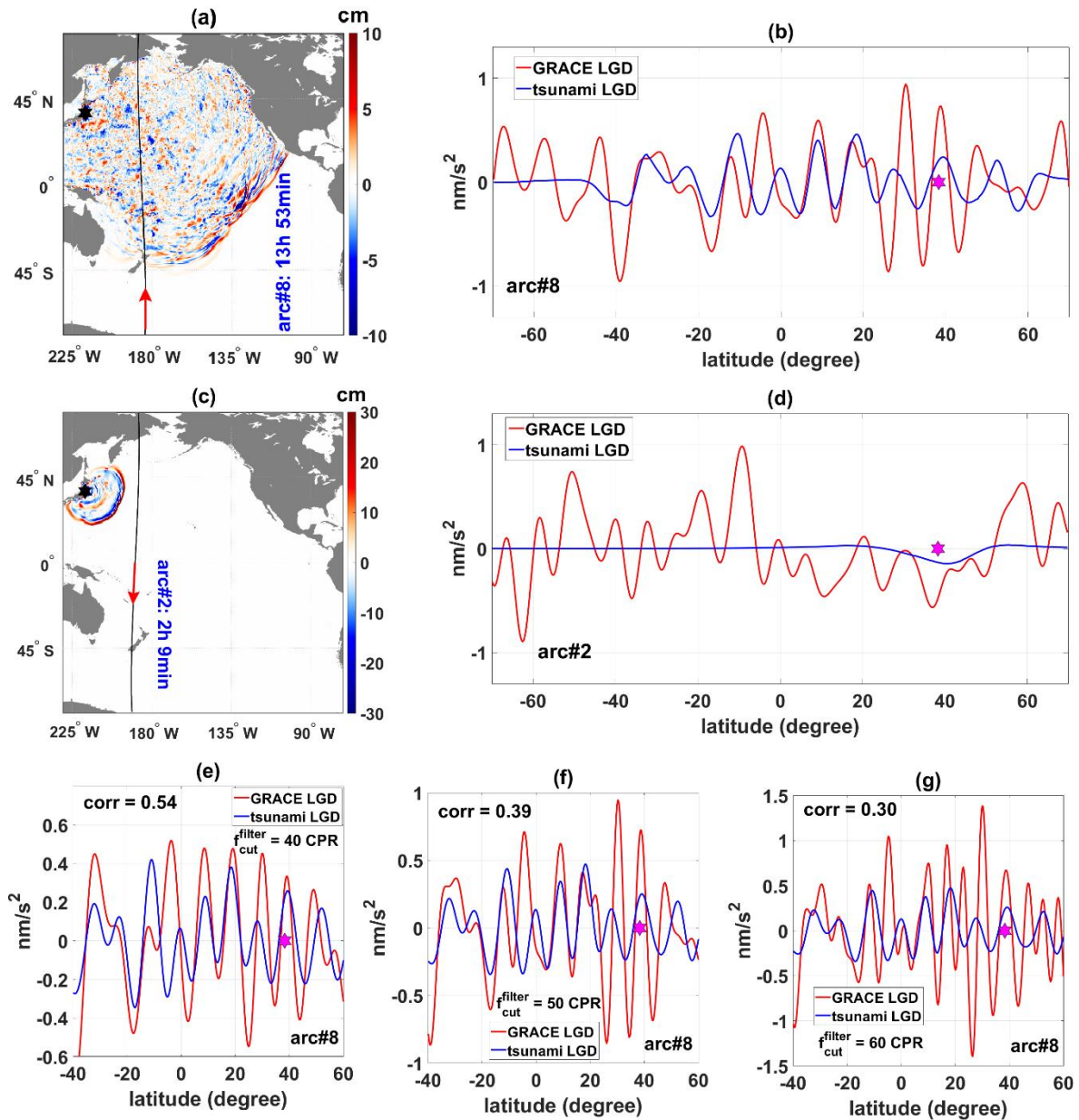


**Figure S16.** GRACE possible detection of tsunami triggered by the 2011 Tohoku earthquake which occurred on 11 March 2011 05:46:24 UTC. **(a)** GRACE ascending track 13 hours and 53 minutes after the earthquake rupture along with the tsunami wave field at the same time. **(b)** Comparison between the GRACE observed (low-pass filtered at 50 CPR, shown in *red*) and tsunami simulated (*blue*) LGD along the ascending track shown in panel (a). **(c)** The closest GRACE descending track over 24 hours after the earthquake which happened 2 hours and 9 minutes after the event along with the tsunami wave field at the same time. **(d)** Comparison between the GRACE observed and tsunami simulated LGD along the descending track shown in (c). **(e)**, **(f)**, and **(g)** Comparison of the GRACE (*red*) and tsunami (*blue*) LGD from latitude 40°S and 60°N both low-pass filtered at 40, 50, and 60 CPR, respectively. The star indicates the epicenter of earthquake.

**Table S1.** Correlation and RMS reduction of GRACE data with the tsunami model along the arc which the detection occurred (columns 2 and 3). To show the statistical significance of these values, we report the correlation and RMS reduction of another GRACE arc (with ~12 hours time difference) covering the same region with the tsunami model (columns 4 and 5).

<b>2004 Sumatra</b>	<b>Asc. arc ~1 hour after the EQ along which detection occurred</b>		<b>Desc. arc ~13 hours after the EQ covering the same region</b>	
	Corr.	RMS reduction	Corr.	RMS reduction
	0.98	0.76	-0.50	-1.84
<b>2010 Maule</b>	<b>Asc. arc ~14 hours after the EQ along which detection occurred</b>		<b>Desc. arc ~2 hours after the EQ covering the same region</b>	
	Corr.	RMS reduction	Corr.	RMS reduction
	0.90	0.6	-0.3	-0.53
<b>2011 Tohoku</b>	<b>Desc. arc ~3 hours after the EQ along which detection occurred</b>		<b>Asc. arc ~15 hours after the EQ covering the same region</b>	
	Corr.	RMS reduction	Corr.	RMS reduction
	0.80	0.4	-0.16	-0.67

**Table S2.** Correlation and RMS reduction of GRACE data with the tsunami model along the arc which detection occurred (columns 2 and 3). To demonstrate the statistical significance of these values, we extracted all GRACE arcs in December 2004, February 2010 and March 2011 which were located within 10° (in longitude) from the arc associated with the detection. We found about 70 arcs for each case. We then computed the correlation and RMS reduction of GRACE data along these arcs with the tsunami model. Mean of correlation and RMS reduction for all the GRACE arcs covering the same region is reported in columns 4 and 5.

<b>2004 Sumatra</b>	<b>Asc. arc ~1 hour after the EQ along which detection occurred</b>		<b>All arcs within 10° from the arc along which detection occurred</b>	
	Corr.	RMS reduction	Mean of Corr. for all arcs	Mean of RMS reduction for all arcs
	0.98	0.76	-0.07	-4.02
<b>2010 Maule</b>	<b>Asc. arc ~14 hours after the EQ along which detection occurred</b>		<b>All arcs within 10° from the arc along which detection occurred</b>	
	Corr.	RMS reduction	Mean of Corr. for all arcs	Mean of RMS reduction for all arcs
	0.90	0.6	-0.05	-0.90
<b>2011 Tohoku</b>	<b>Desc. arc ~3 hours after the EQ along which detection occurred</b>		<b>All arcs within 10° from the arc along which detection occurred</b>	
	Corr.	RMS reduction	Mean of Corr. for all arcs	Mean of RMS reduction for all arcs
	0.80	0.4	-0.02	-0.35